Non-Newtonian viscosity of atomic fluids in shear and shear-free flows

Carlo Pierleoni and Jean-Paul Ryckaert*
Physics Department, Code Postal 223, Université Libre de Bruxelles, 1050 Brussels, Belgium
(Received 12 March 1991)

Simple shear and various simple shear-free flows with constant traceless velocity gradient are simulated at the microscopic level for an atomic fluid at a single state point. The dependence of the viscosity upon the strain rate is obtained for each specific flow and analyzed on the basis of the retarded motion expansion of the nonequilibrium pressure tensor. Within the investigated range of strain rate, the pressure and the internal energy follow a linear behavior in terms of the second scalar invariant of the strain-rate tensor which, as expected by symmetry, is common to all flows.

PACS number(s): 47.50.+d, 66.20.+d, 61.20.Ja, 62.10.+s

In this paper we present nonequilibrium molecular-dynamics (NEMD) results on the rheological behavior of an atomic fluid. We performed a series of experiments where the fluid, at a single state point, is subjected to different homogeneous steady flows with zero divergence, implying a constant volume steady deformation of the system. Both shear and shear-free flows were considered for increasing strain rate.

The viscosity in planar Couette (simple shear) flow and in planar elongational flow exhibits strain-rate thinning. In uniaxial elongational flow we observe strong thinning for uniaxial stretching and weak thickening for biaxial stretching (uniaxial compression), while the strain-rate derivative of the viscosity is continuous and negative for vanishing elongational rates. In the linear regime all viscosities reduce, within statistical errors, to the Newtonian viscosity η_0 which was independently computed by its Green-Kubo formula.

When the above viscosities are expressed in terms of the second scalar invariant of the strain-rate tensor [denoted by Γ_2 and defined in (3)], similar behaviors are observed. The viscosity data in planar flows fall on the same curve within statistical errors. Moreover, in uniaxial elongational flow, the viscosities relative to stretching and compressional cases lie symmetrically above and below the planar flow data. For all flows, the pressure and the internal energy show, in the investigated strain-rate domain, an apparent universal linear behavior in terms of Γ_2.

Since all flows considered are characterized by a small Deborah number ($D<0.2$), our results on viscosity can be interpreted on the basis of the retarded motion expansion (RME) [1a] and provide a quantitative estimate of some low-order coefficients. Consequently, we are able to specify the range of validity of low nth-order fluid approximations for the viscosity material function. In particular, this analysis suggests that the observed similarities are restricted to a limited range of strain rates. Unfortunately, it remains impossible to compare the simulation results with real experiments, as the non-Newtonian effects in atomic fluids appear at experimentally inaccessible high strain rates ($\approx 10^{12}\,\mathrm{sec}^{-1}$).

The rheology of atomic fluids has already been the object of many NEMD experiments. Very precise results on the strain-rate dependence of shear viscosity are available [2–4], but an interpretation in terms of classical rheological theories is still lacking. Results on shear-free flows have also been published in an attempt to give a more complete description of the rheological behavior [5,6], but they remain very preliminary because no consistent picture could be inferred. In the present work, a unified interpretation of NEMD results on different flows is provided in the context of numerical simulation at the molecular level. It leads to numerical estimates of some low-order RME coefficients for a specific microscopic model: this is not only of academic interest, as kinetic-theory predictions of these coefficients have already been derived for various molecular models of polymer melts and solutions [1].

In our simulations, we deal with steady velocity fields $\mathbf{v}(\mathbf{r})$ with the traceless gradient homogeneous in space. For the sake of simplicity, the notation of Ref. [1] will be adopted as much as possible throughout this paper. Denoting by $\dot\gamma$ and $\dot\epsilon$ the shear rate and the elongational rate, respectively, all flows considered in this work can be expressed in terms of the velocity gradient

$$\nabla\mathbf{v}=\begin{bmatrix}-\dot\epsilon(1+b)/2 & 0 & 0\\ \dot\gamma & -\dot\epsilon(1-b)/2 & 0\\ 0 & 0 & \dot\epsilon\end{bmatrix}, \qquad (1)$$

to which corresponds the strain-rate tensor

$$\overleftrightarrow{\dot\gamma}=[(\nabla\mathbf{v})+(\nabla\mathbf{v})^T] =\begin{bmatrix}-\dot\epsilon(1+b) & \dot\gamma & 0\\ \dot\gamma & -\dot\epsilon(1-b) & 0\\ 0 & 0 & 2\dot\epsilon\end{bmatrix}. \qquad (2)$$

The planar Couette flow (shear flow) corresponds to $\dot\gamma\neq0$ and $\dot\epsilon=0$. The elongational flows (shear-free flows) are given by $\dot\gamma=0$ and $\dot\epsilon\neq0$, with parameter $b=1,0$ corresponding to planar and uniaxial elongational flows, respectively. In the last case $\dot\epsilon>0$ corresponds to uniaxial stretching and $\dot\epsilon<0$ to uniaxial compression. The scalar invariants of the strain-rate tensor, defined as

$$\Gamma_1=\mathrm{tr}\overleftrightarrow{\gamma},\quad \Gamma_2=\mathrm{tr}(\overleftrightarrow{\gamma}\cdot\overleftrightarrow{\gamma}),\quad \Gamma_3=\mathrm{tr}(\overleftrightarrow{\gamma}\cdot\overleftrightarrow{\gamma}\cdot\overleftrightarrow{\gamma}) \tag{3}$$

are summarized in Table I for all flows. Note that $\Gamma_1=0$ and $\Gamma_2>0$ for all flows Γ_3 is zero for the planar flows, and in the uniaxial elongational flow it has the sign of $\dot{\epsilon}$. In Table I, we also mention the usual definition of the generalized viscosity specific for each flow. For vanishing strain rates, Newton's law implies [1(a)]

$$\lim_{\dot{\gamma}\to 0}\eta(\dot{\gamma})=\lim_{\dot{\epsilon}\to 0^{\pm}}\frac{\overline{\eta}(\dot{\epsilon},b)}{3+b}=\eta_0\,, \tag{4}$$

where η and $\overline{\eta}$ are the shear and elongational viscosities respectively.

We considered a Weeks-Chandler-Andersen [7] fluid [purely repulsive Lennard-Jones (LJ) pair interactions truncated at $r_c=2^{1/6}\sigma$] composed of $N=864$ point particles. Throughout this work, we dealt with a single thermodynamic state point defined by the density $\rho=0.8\sigma^{-3}$ and the temperature $T=1.5\varepsilon/k_B$ where σ and ε are the usual LJ parameters and k_B is the Boltzmann constant.

In our experiments we exploited the *dynamical* NEMD method [8,9], which follows the transient behavior of the fluid from equilibrium until the onset of the stationary state corresponding to the applied homogeneous and constant velocity field. A constant-density, constant-temperature stationary state was indeed observed because (i) our flows had zero divergence and (ii) heat was removed homogeneously from the system by a thermostat. The plateau value of the elements of the viscous pressure tensor $\overleftrightarrow{\tau}$ (called a stress tensor in Ref. [1]) was used to give an estimation of the generalized viscosity and the deviation of the pressure from its equilibrium value $\Delta p=\frac{1}{3}(\tau_{xx}+\tau_{yy}+\tau_{zz})$.

In these experiments we used a *synthetic* NEMD algorithm (known as the SLLOD algorithm [10,11]), in which the homogeneous velocity gradient is induced by a fictitious field at the molecular level. The temperature was controlled by a Nosé-Hoover (NH) thermostat [12]. The velocity gradient was taken to be $\nabla\mathbf{v}\Theta(t)$, where $\nabla\mathbf{v}$ is the constant tensor fixed by a particular form of (1) and where $\Theta(t)$ is a unit step function in time. The second-order differential equations [9,10], derived from the SLLOD equations have the form

$$\ddot{\mathbf{r}}_i=\frac{\mathbf{F}_i}{m}+(\nabla\mathbf{v})^T\cdot\mathbf{r}_i\delta(t)+(\nabla\mathbf{v})^T\cdot[(\nabla\mathbf{v})^T\cdot\mathbf{r}_i]$$
$$-\xi[\dot{\mathbf{r}}_i-(\nabla\mathbf{v})^T\cdot\mathbf{r}_i] \tag{5}$$

for an atom i of mass m with Cartesian coordinates $\mathbf{r}_i$.

The first term on the right-hand side of (5) is the usual acceleration of microscopic origin due to the total intermolecular force $\mathbf{F}_i$. The second term is the instantaneous acceleration that must be applied at time $t=0$ in order to initialize the velocity field of the system. The third term, which corresponds to the material time derivative of the local macroscopic velocity field, forces a fluid element to follow the streamlines of the imposed velocity field. At the same time, the "molecular-dynamics box" deforms according to the flow but remains the unit cell of an infinite periodic system [9]. The last term represents the effect of the thermostat [12]. It introduces an extra variable ξ that obeys the differential equation $d\xi/dt=[K-(3N-1)k_BT]/Q$, where K is twice the kinetic energy computed by the peculiar velocities (the thermal part of the velocities out of the local velocity field) and Q is a parameter that controls the efficiency of the thermostat. The equations of motion (5) were integrated by the velocity version of the Verlet algorithm [13] with a time step $h=0.005\sigma(m/\epsilon)^{1/2}$. The thermostat coupling parameter was chosen to get $Q/(3N-1)=0.008m\sigma^2$.

The transient fluid behavior was obtained by averaging nonequilibrium trajectories of time length $1.0\sigma(m/\varepsilon)^{1/2}$ over many (typically 1000) initial equilibrium configurations. These were generated by a separate canonical equilibrium MD simulation (performed in the absence of flow but in the presence of the thermostat). In the linear regime (the Newtonian regime) the subtraction technique [14] was applied to extract the signal from the noise. In all cases, the onset of the plateau in the viscosity took place around $t=0.4\sigma(m/\epsilon)^{1/2}$ and, within the explored range of the elongational rate, the deformation of the box never caused opposite sides to come closer than 5σ.

The data on the generalized viscosities for all flows are shown in Fig. 1, normalized by a factor $3+b$ for elongational flows so as to display relationship (4) in the zero-strain-rate limit. An asterisk is used to indicate quantities expressed in the usual LJ units. The Green-Kubo value $\eta_0^*=1.71\pm0.01$ was evaluated using an equilibrium trajectory of 4×10^6 steps. This value is indeed compatible with all extrapolated generalized viscosities for the vanishing strain rate. Note that, by symmetry, the viscosity in planar flows is independent of the sign of the strain rate. In Fig. 2, we plot the viscosity in the two planar flows and the two branches of the elongational viscosity in uniaxial elongational flow (uniaxial compression and uniaxial stretching) against the second scalar invariant Γ_2. Within statistical errors, we observe a common curve for planar Couette flow and planar elongational

TABLE I. Strain-rate scalar invariants and generalized viscosity for shear and shear-free (elongational) flows : planar and uniaxial elongational flows correspond to $b=1$ and 0, respectively. $\dot{\gamma}$ and $\dot{\epsilon}$ are the shear and elongational rates, respectively, and $\overleftrightarrow{\tau}$ is the viscous pressure tensor.

Flow	$\dot{\gamma}$	$\dot{\epsilon}$	Γ_1	Γ_2	Γ_3	Generalized viscosity
Shear	$\neq 0$	0	0	$2\dot{\gamma}^2$	0	$\eta(\dot{\gamma})=-\tau_{xy}/\dot{\gamma}$
Shear-free	0	$\neq 0$	0	$2(3+b^2)\dot{\epsilon}^2$	$6(1-b^2)\dot{\epsilon}^3$	$\overline{\eta}(\dot{\epsilon},b)=-(\tau_{zz}-\tau_{xx})/\dot{\epsilon}$

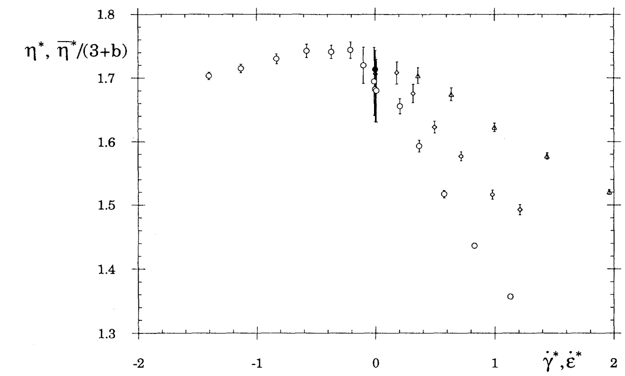

FIG. 1. Reduced shear viscosity η^* and elongational viscosities $\bar{\eta}^*/(3+b)$ vs reduced shear rate $\dot{\gamma}^*$ and elongational rate $\dot{\epsilon}^*$, respectively. All data on planar Couette (△), planar elongational (◇) and uniaxial elongational flows (○) are shown together with the Green-Kubo (●) estimate η_0^*.

flow lying midway between the uniaxial elongational flow branches.

In all flows, the relative change of the viscosity with strain rate suggests that we are exploring small deviations from the linear Newton's law. A measure of such nonlinearities for a particular fluid-flow system is the Deborah number [1(a)] D defined as the ratio of the stress response time of the fluid λ to the characteristic time of the flow τ_F. We estimate $\lambda \simeq 0.06$ from the time integral of the normalized equilibrium stress-stress correlation function (stress-relaxation modulus). As we consider steady flows, $\sqrt{\Gamma_2}$ is a natural choice for τ_F so that $D<0.2$ for all our experiments. In this range of D, our results can be interpreted in the framework of the retarded motion expansion [1(a)], which relates the viscous

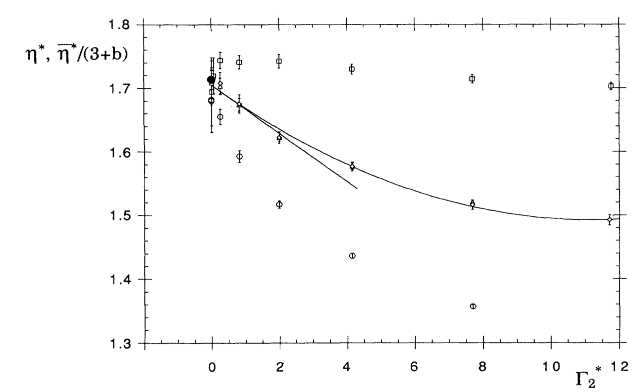

FIG. 2. Reduced shear viscosity η^* and elongational viscosities $\bar{\eta}^*/(3+b)$ vs the reduced second scalar invariant of the strain-rate tensor Γ_2^*. The symbols for planar flows and Green-Kubo data are as in Fig. 1. The uniaxial elongational viscosity is now plotted in two branches corresponding to uniaxial extension (○) and uniaxial compression (□). The solid curve is a fit $\bar{\eta}^*/4=a+b\Gamma_2^*+c(\Gamma_2^*)^2$ on planar elongational data which provides $a=1.705\pm0.008$, $b=(-3.8\pm0.3)\times10^{-2}$, and $c=(1.7\pm0.3)\times10^{-3}$. The straight line and the solid curve represent third and fifth-order fluid models, respectively.

pressure tensor to the set of convected time derivatives of the strain-rate tensor. These are defined recursively as

$$\overleftrightarrow{\gamma}_{(1)}=\overleftrightarrow{\gamma}\ , \tag{6a}$$

$$\overleftrightarrow{\gamma}_{(n+1)}=\frac{D}{Dt}(\overleftrightarrow{\gamma}_{(n)})-[(\nabla\mathbf{v})^T\cdot\overleftrightarrow{\gamma}_{(n)}+\overleftrightarrow{\gamma}_{(n)}\cdot(\nabla\mathbf{v})] \quad (n\geq1)\ , \tag{6b}$$

where $D/Dt=(\partial/\partial t+\sum_\alpha v_\alpha\partial/\partial r_\alpha)$ is the material time derivative that vanishes for steady homogeneous flows. Noting that $\overleftrightarrow{\gamma}_{(n)}$ is of order n in the strain rate, the RME for an incompressible fluid, written here explicitly up to the third order, is

$$\begin{aligned}\overleftrightarrow{\tau}=-[&b_1\overleftrightarrow{\gamma}_{(1)}+b_2\overleftrightarrow{\gamma}_{(2)}+b_{11}(\overleftrightarrow{\gamma}_{(1)}\cdot\overleftrightarrow{\gamma}_{(1)})+b_3\overleftrightarrow{\gamma}_{(3)}\\&+b_{12}(\overleftrightarrow{\gamma}_{(1)}\cdot\overleftrightarrow{\gamma}_{(2)}+\overleftrightarrow{\gamma}_{(2)}\cdot\overleftrightarrow{\gamma}_{(1)})\\&+b_{1:11}(\overleftrightarrow{\gamma}_{(1)}:\overleftrightarrow{\gamma}_{(1)})\overleftrightarrow{\gamma}_{(1)}+\cdots]\ ,\end{aligned} \tag{7}$$

where the coefficients b_α are material parameters. According to the current terminology, an nth-order fluid is defined by the constitutive relation (7) truncated at order n. It is then straightforward [1(a)], for a given flow, to write down the viscosity of the nth-order fluid in terms of the material coefficients b_α. For any specific velocity gradient (1), the tensors $\overleftrightarrow{\gamma}_{(m)}$ $(m\leq n)$ are computed according to (6) and substituted in (7). Then the viscosity expression follows from its definition in terms of $\overleftrightarrow{\tau}$ (see Table I). For the third-order fluid, the shear and elongational viscosities in planar and in uniaxial elongational flow are, respectively,

$$\begin{aligned}\eta(\dot{\gamma})&=b_1-(b_{12}-b_{1:11})2\dot{\gamma}^2\\&=b_1-(b_{12}-b_{1:11}\Gamma_2\ ,\end{aligned} \tag{8}$$

$$\begin{aligned}\bar{\eta}(\dot{\epsilon},1)/4&=b_1-(b_{12}-b_{1:11}-b_3/2)8\dot{\epsilon}^2\\&=b_1-(b_{12}-b_{1:11}-b_3/2)\Gamma_2,\end{aligned} \tag{9}$$

$$\begin{aligned}\bar{\eta}(\dot{\epsilon},0)/3&=b_1+(b_{11}-b_2)\dot{\epsilon}-(b_{12}-b_{1:11}-b_3/2)6\dot{\epsilon}^2\\&=b_1+(b_{11}-b_2)\dot{\epsilon}-(b_{12}-b_{1:11}-b_3/2)\Gamma_2\ ,\end{aligned} \tag{10}$$

where the second scalar invariant Γ_2 for each specific flow is reported in Table I. From (9) and (10) we see that in terms of Γ_2, the viscosity in planar elongational flow $\bar{\eta}(\dot{\epsilon},1)/4$ and the symmetric part of the viscosity in uniaxial elongational flow $\bar{\eta}(\dot{\epsilon},0)/3$ are equivalent, in agreement with our earlier remark (Fig. 2). However, a more general analysis suggests that this property does not hold for an nth-order fluid with $n>4$. As concerns the comparison between $\eta(\dot{\gamma})$ and $\bar{\eta}(\dot{\epsilon},1)/4$ in terms of Γ_2, we see from (8) and (9) that already for the third-order fluid both expressions differ by $b_3/2\ \Gamma_2$. Second-order polynomial fits of the data for planar Couette and planar elongational flow in terms of Γ_2 give $b_{12}-b_{1:11}=(4.1\pm0.4)10^{-2}$ and $b_{12}-b_{1:11}-b_3/2=(3.8\pm0.3)\times10^{-2}$. This leads to the conclusion that the size of b_3 is within statistical errors. Figure 2 shows the fit on planar elongational flow data, for which the second-order coefficient turns out to be

$(1.7\pm0.3)\times10^{-3}$. The straight line represents the polynomial fit up to the linear term, showing that a third-order fluid model is able to reproduce the nonlinear viscosity up to $D\simeq0.1$ ($\Gamma_2=0.2$), while a fifth-order fluid is necessary to reach $D\simeq0.2$.

The pressure and the internal energy per particle deviated from their equilibrium value during our transient experiments. While the instantaneous viscosity response rapidly reached a well-defined plateau, these thermodynamic quantities underwent an initial rise, followed by long-lived damped oscillations still present at $t^*=1$, which are possibly due to interference from the thermostatting mechanism. We therefore measured the stationary-state pressures and internal energies from the apparent asymptotic mean without trying to estimate the associated errors. In Fig. 3 these quantities are plotted versus Γ_2 for all shear and shear-free flows showing a common linear behavior. This can be explained by symmetry arguments if we assume that the nonequilibrium deviation of an arbitrary scalar quantity can be formally developed in a power series of the perturbation. For an isotropic system subjected to a tensorial perturbation, the nth coefficient of the expansion must be isotropic tensors of rank $2n$. If we consider traceless velocity gradients and if, following the rheological invariance principle [1(a)], we require that a purely rotational flow (antisymmetric velocity gradient) must not induce any nonequilibrium deviation, it follows that the first nonvanishing term in the expansion is, for all flows, a second-order term linear in Γ_2. For the pressure, the slope α could

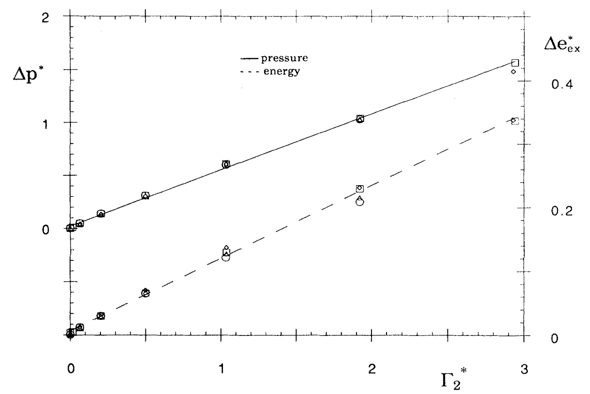

FIG. 3. Variation of the reduced pressure and the reduced internal energy per particle in various flows as a function of Γ_2^*. Symbols are as in Fig. 2.

easily be related to the coefficients of the RME for compressible fluids. A RME global analysis of our results, including additional data on normal stress effects, will appear separately [15].

We are most grateful to G. Ciccotti and Ph. Boulanger for useful discussions and suggestions. We thank Donal McKernan for a critical reading of the manuscript. The research of C. Pierleoni is supported by the European Community under Contract No. SC1*0059. A generous allocation of computer time was provided by the CNR-CRAY Group on Statistical Mechanics.

*Author to whom correspondence should be addressed: Physics Department, CP 223, Campus Plaine, Université Libre de Bruxelles, Boulevard du Triomphe, 1050 Brussels, Belgium.

[1] (a) R. B. Bird, R. C. Armstrong, and O. Hassager, *Dynamics of Polymeric Liquids,* 2nd ed. (Wiley Interscience, New York, 1987), Vol. 1; (b) R. B. Bird, C. F. Curtiss, R. C. Armstrong, and O. Hassager, *Dynamics of Polymeric Liquids,* 2nd ed. (Wiley Interscience, New York, 1987), Vol. 2.

[2] D. J. Evans, G. P. Morriss, and L. M. Hood, Mol Phys. **68**, 637 (1989).

[3] J. P. Ryckaert, A. Bellemans, G. Ciccotti, and G. V. Paolini, Phys. Rev. Lett. **60**, 128 (1987).

[4] M. Ferrario, G. Ciccotti, B. L. Holian, and J. P. Ryckaert, Phys. Rev. A (to be published).

[5] D. M. Heyes, Chem. Phys. **98**, 15 (1985); Phys. Lett. **115**, 42 (1986).

[6] M. W. Evans and D. M. Heyes, Mol. Phys. **69**, 241 (1990).

[7] J. P. Hansen and I. R. McDonald, *Theory of Simple Liquids,* (Academic, London, 1986).

[8] J. P. Ryckaert, A. Bellemans, G. Ciccotti, and G. V. Paolini, Phys. Rev. A **39**, 259 (1989).

[9] J. P. Ryckaert, Ber. Bunsenges. Phys. Chem. **94**, 256 (1990); H. Xu and J. P. Ryckaert, J. Chem. Phys. **93**, 5234 (1990).

[10] A. J. C. Ladd, Mol. Phys. **53**, 459 (1984).

[11] D. J. Evans and G. P. Morriss, Comp. Phys. Rep. **1**, 299 (1984).

[12] B. L. Holian and D. J. Evans, J. Chem. Phys. **83**, 3560 (1985), and references cited therein.

[13] W. C. Swope, H. C. Andersen, P. H. Berens, nd K. R. Wilson, J. Chem. Phys. **76**, 637 (1982).

[14] G. Ciccotti, G. Jacucci, and I. R. McDonald, J. Stat. Phys. **21**, 1 (1979).

[15] C. Pierleoni and J. P. Ryckaert (unpublished).